High-Efficiency Slot Array Antenna Fed by a Microstrip Line to ESIW Transition for X-band Applications

Ahmad Parsa[1], Pejman Rezaei[1]*, Ali Amne Elahi[1], Zahra Mousavirazi[2]

Abstract— **In this manuscript, a planar slot array antenna with an innovative method is designed at a 10 GHz centrecentre frequency. The designed antenna is manufactured on PCB. In this antenna, the input power enters the microstrip line, then this power enters the empty SIW (ESIW) structure via transition and then this structure fed the eight radiation slots on the antenna. The geometry of the ESIW structure is designed as a tapered substrate, which eliminates the interference effects of higher-order modes with the dominant mode, thus providing extreme antenna radiation power. The techniques used in feeding the radiation elements have acceptable effects on the impedance bandwidth and radiation efficiency. The designed antenna feeding bandwidth is 2 GHz, also the antenna fractional bandwidth is 7.5%. All simulations were performed using CST Studio Suite software. The antenna radiation gains and efficiency are 13.8 dB and about 92% at 10 GHz, respectively. The configured antenna dimension is 222.75 × 40 × 4.4 mm^3.**

Index Term: **Microstrip; tapered substrate; slot array antenna; substrate integrated waveguides (SIW); Empty SIW; via transition.**

I. INTRODUCTION

Due to the rapid move toward 5G and 6G technologies , the expansion of data transmission in wireless communication, the attention of investigatorshas been directed to the function of the antenna as the main part of a communication system [1]. For this reason, microstrip structures as a low-cost and integrable platform have been developed in different types of communication equipmentequipment such as antennae [2-4], filters [5-7], absorbers [8-11], sensor [12-16] and oscillator [17-19].
Despite the numerous and well-known advantages of the microstrip structure, the desire to use other existing structures such as different types of substrate-integrated waveguides (SIW), has led RF circuit designers to hybrid structures. These composite structures require proper connections and transitions [20].

In recent years, slot array antennas have received much attention in radar and monopulse applications due to their simple geometry and high efficiency [21-23]. In this class of applications, non-planar structures such as waveguides and coaxial lines are used, which are bulky and costly [24-27]. Planar transmission lines have been proposed to solve the challenges of non-planar structures [28-31].

The integrated planar and non-planar transmission line requires be careful machining process as well as mass manufacture at microwave and millimeter wave frequencies is expensive. Today has been designed inexpensive and compact systems such as SIWs that have been highly regarded by researchers [32-34]. SIWs have been used due to their low-cost construction and higher quality factors than planar and non-planar transmission lines. One of the features of this technology is that it uses the advantages of waveguides and microstrip, but it does not include the problems caused by them [35-39]. The SIW structures are composed of a dielectric and metal vias, which form the overall wall of the structure. The utilization of dielectric in these structures imposes constraints on the structure. One of these constraints is the increase in losses in the structure, which led to a decrease in the gain of antennas based on these structures.

Another constraint that can be expressed for this type of structure is the cost of using a dielectric for these structures to solve the problem of losses in SIW structures, new structures have been introduced in which air has been used instead of dielectric, which is why these structures are called air-filled SIW or empty SIW (ESIW).

The advantages of using ESIW structures instead of SIW are lower losses, higher quality factors, and an easier manufacturing process. ESIW structures compared to classic waveguide structures can integrate with low prices, also these structures have all the benefits of the classical waveguide and SIW structures [40-43]. Also, slot array antenna based on ESIW structure for 5-G, and MIMO applications are introduced in [44, 45].

This planned antenna is a suitable array for X-band radar applications due to its specifications. This article is separated into the following sections: First part, the performance of the feed is examined, with a parametric study. The next section compares the simulation and fabrication results and compares the antenna with previous work. Finally, the general conclusion of the work is stated.

II. TOPOLOGY OF FEEDING STRUCTURE

Three components make up the suggested slot array antenna power supply. A microstrip line serves as the first component and allows input power to enter the structure. The power then uses a transition to enter the ESIW structure. The outside substrate contains the integrated microstrip line, which is coupled to the inside substrate by a transition and fastened to the PEC plate using radiating slots. The dielectric tapper shape causes more coupling as well as more power transfer to the radiation slots. The purpose of investigating the feeding structure is to obtain the effect on the slot array performance. The feeding structure dimension has been displayed in Fig. 1.

1: Electrical and Computer Engineering Faculty, Semnan University, Semnan, Iran.
2: Institut National de la Recherche Scientifique, University of Quebec, Montreal, QC, Canada.
Corresponding author: prezaei@semnan.ac.ir

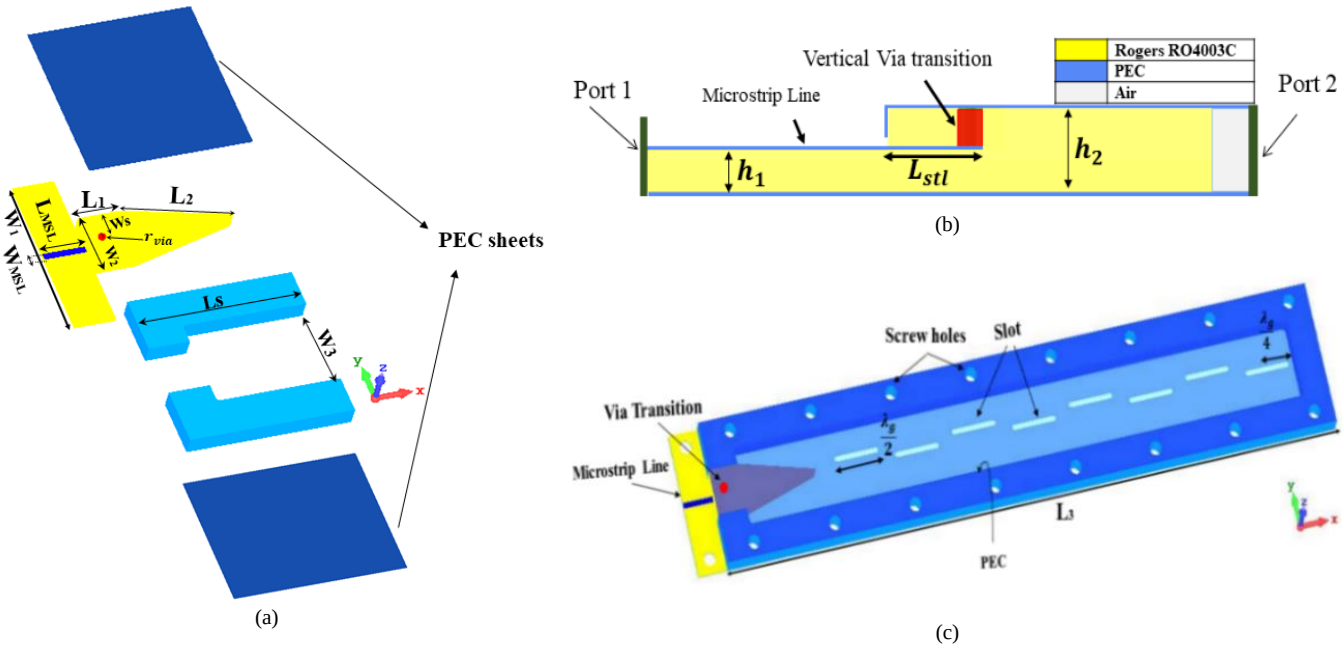

Fig. 1. Details of the proposed planar slot array antenna with feeding structure dimensions: (a) exploded view, (b) side view, (c) 3-D overview.

The equations (1) and (2) have been used to calculate the effective width and relative permittivity of the microstrip line. To obtain the microstrip line impedance used equations in [46]

$$W_{eff} = 0.536\, W_{MSL} + 0.6 \tag{1}$$

$$\varepsilon_{r,eff} \cong 0.475\, \varepsilon_r + 0.67 \tag{2}$$

$$Z_{o1} = \frac{1}{2\pi} \times \sqrt{\frac{\mu}{\varepsilon_o \varepsilon_{reff}}} \ln\left(\frac{4h_1}{W_{eff}}\right) \tag{3}$$

The calculated values of equations (1) and (3) and the structure dimensions are given in Table I. The dielectric material used is Rogers RO4003C with a relative permittivity of (ε_r = 3.55). The heights of the microstrip line dielectric and the proposed ESIW dielectric are 0.8 and 2.4 mm, respectively. The conductor thickness is 0.035 mm in the full wave simulation.

TABLE I
The Planned Antenna Dimensions.

Param	Value	unit	Param	Value	unit
L1	10	*mm*	ε_{reff}	2.75	F/m
L2	25.5	*mm*	h1	0.8	*mm*
rvia	0.5	*mm*	Wmsl	1.61	*mm*
Lstl	3.45	*mm*	Lmsl	10	*mm*
h2	2.4	*mm*	W1	40	*mm*
ZO1	50	*Ω*	W2	12.7	*mm*
Ls	40	*mm*	Ws	6.35	*mm*
L3	212.75	*mm*	W3	21.7	*mm*

According to the structure geometry shown in Fig. 1, the input power passing through the transmission lines transfers to the and dielectric environment by using the design via transition. An overview of the planned slot array structure is presented in Fig. 1(c). The λ_g can be obtained from equation 4.

$$\lambda_g = \frac{2\pi}{\sqrt{\left(\frac{\varepsilon_r (2\pi . f)^2}{c^2}\right) - \left(\frac{\pi}{a}\right)^2}} \tag{4}$$

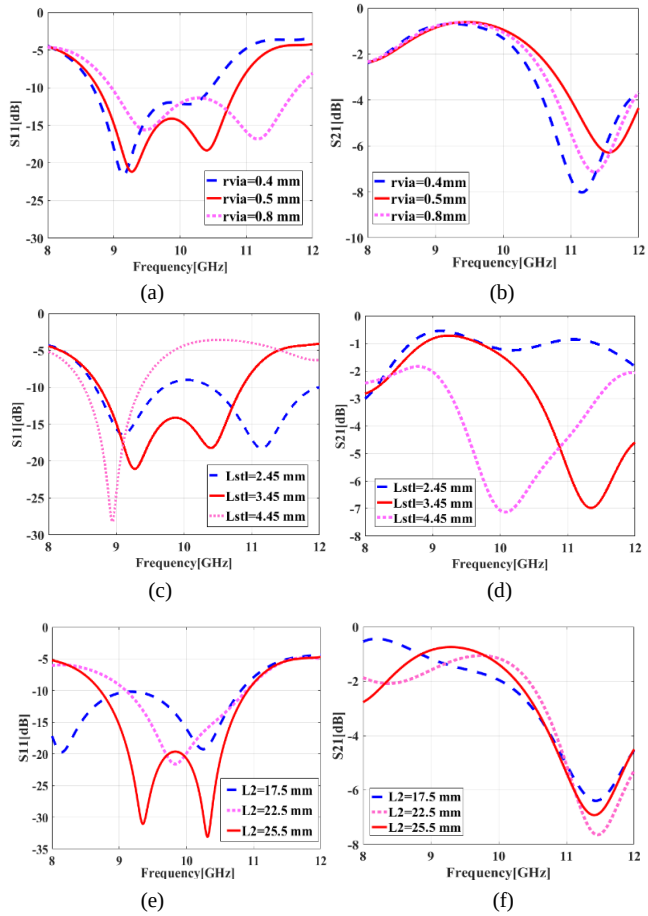

Fig. 2 Scattering parameters (S_{11}, S_{21}) with the variation of (a, b) via radius, (c, d) L_{stl}, (e, f) taper dielectric length.

A parametric investigation was performed on the transmission line parameters to adjust the operating frequency more precisely. The designed antenna is simulated with full-wave CST software. The results are reported based on the variation of antenna dimension (width and length) in Fig. 2.

The results related to the via radius variation are reported in Figure 2(a, b). The S11 response best obtained with 2 GHz bandwidth for via radius is 0.5 mm. In Figure 2(c, d), by increasing or decreasing the Lstl that causes a change in via transition position as a result, it has changed the return loss and insertion loss. When the value of Lstl is 3.45 mm, S11 and S21 are -15 dB and -3 dB, respectively. In Figure 2(e, f), by changing the L_2 length, the appropriate S_{11} value is obtained. When the length of the taper dielectric section is 25.5 mm, impedance bandwidth, and return loss are 2.1 GHz and -20 dB, respectively.

In this parametric study, the change in via transition position and the taper dielectric section length (L2) has a greater effect on this design. The distance of each slot with the next slot is set to λg/2. Furthermore, the last slot to the side wall distance is λg/4.

The slot array antenna bandwidth with the suggested feeding structure is 750 MHz, as indicated in Figure 2C, where the simulated values of S11 are obtained at 10 GHz. Additionally, the efficiency and radiation gain are 92% and 13.8 dBi, respectively.

The efficiency of aperture and radiation are two features to obtain a high radiation gain. The antenna aperture efficiency can be obtained from equation (5):

$$\eta_a = \frac{G \times {\lambda_0}^2}{4 \times \pi \times A} \quad (5)$$

Where η_a is the efficiency of the antenna aperture. A, G, and λ_0 are the aperture area, the antenna gains, and the free space wavelength respectively.

The array's physical aperture dimension is 222.75×40 mm^2. The array peak measured gain is 13.8 dB at 10 GHz. It is equal to 20% aperture efficiency.

III. MANUFACTURING PROCESS AND MEASUREMENT RESULTS

Proposed antenna with feeding structure manufactured on PCB. According to the standard available as well as easier embedded of the transmission line inside the substrate, three dielectric layers have been used in the antenna fabrication. In Figure 3a, three layers are coupled on top of each other, and the substrate's thickness value is 0.8 mm. By making regular holes in the second and third layers and with solder wire connected the microstrip line to the conductor plate. Adjusting screws are used to mount the antenna plates on top of each other.

The antenna S-parameters were measured with a network analyzer, Agilent-E8361C PNA, as shown in Fig. 3b. There was an appropriate match between the measurement and the simulation results.

(a)

(b)

Fig. 3 Photograph of the designed array antenna prototype (a) The not assembled layers of structure, (b) S-parameter measurement setup.

In Fig. 4, the S11 value difference between simulation and measurement is less than 5 dB. This difference can be seen in similar research, which is due to defections metallization, and dimensional errors that generally occur during the antenna manufacturing process. Of course, this difference has not caused a noticeable change in the designed frequency band of the proposed antenna.

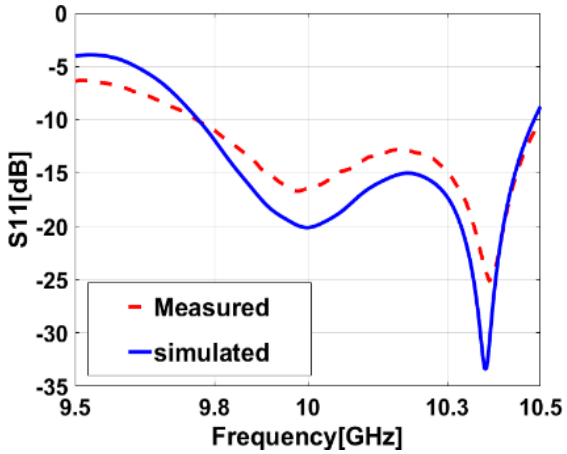

Fig. 4 Comparison of measurement and simulation results of S11.

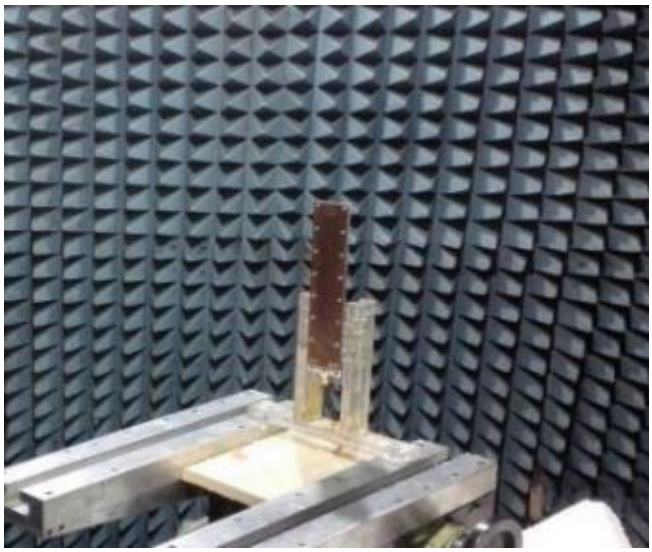

Fig. 5 The radiation pattern measurement in an anechoic chamber.

The manufactured array's radiational pattern was tested in an antenna chamber as shown in Figure 5. The measure and simulation of co- and cross-polar antenna far field radiation patterns for E-plane (EP) and H-plane (HP) at 9.8 GHz and 10 GHz are illustrated in Fig. 6.

The Figs show that, particularly at the antenna back-lobe, there is not much of a discrepancy between the measured and predicted radiation pattern of the antenna.

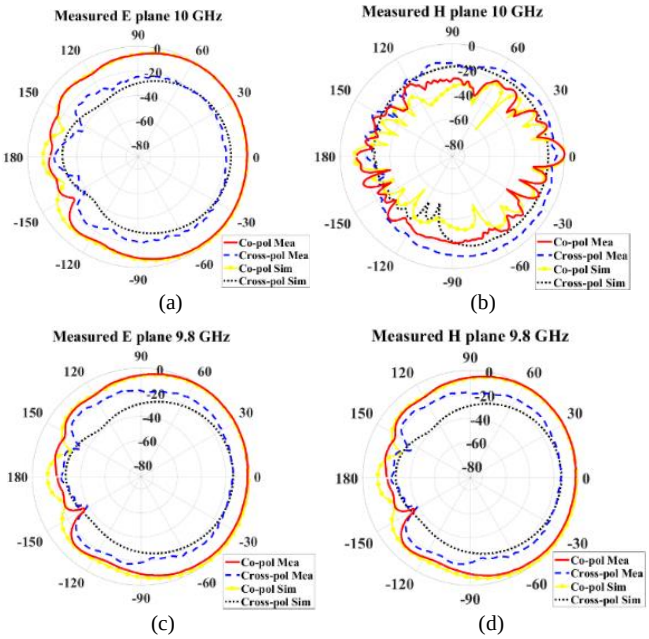

Fig. 6 The simulation and measurement of co-polar and cross-polar radiation patterns: (a) E-Plane @ 9.8 GHz, (b) H-Plane @ 9.8 GHz (c) E-Plane @ 10 GHz, (d) E-Plane @ 10 GHz.

This difference is more tangible in the cross-polar. The main error is related to the unwanted items in the measurement setup, as well as the stretching of the cable at some angles during the test.

TABLE II
Comparison Between the Planned Structure and Recently Published Results.

References	[46]	[47]	[48]	[49]	[50]	[51]	This work
Antenna type	H-plane Horn ESIW	ESIW	SIW cavity backed slot	SIW	SIW	AFSIW	ESIW
Freq. (GHz)	15	28	10.2	24.0	10.0	30.5	10.0
FBW (%)	2.66	6.8	2.57	1.7	6	8.7	7.5
Elements no	NA	NA	1×4	4×32	4×4	1×4	1×8
Efficiency (%)	89	91	85	67	NA	97.4	92
Gain (dBi)	8.55	8.55	7.4	22.8	15.7	11.5	13.5

NA: Not Available

The ESIW structure and the via transition are two characteristics of the feeding structure in this article. Compared with other slot array antennas based on SIW and ESIW, (Table II) the proposed antenna has high radiation efficiency and better impedance bandwidth than the recently published results. In this design the gain and efficiency are better than in other references, however, the design frequency is at 10 GHz.

The feeding structure is an appropriate candidate for engendering many applications, which can straightforwardly be applied in corporate feed and greater arrays for microwave devices. This feeding structure, can be generalized to higher frequencies such as 5G applications.

IV. CONCLUSION

A novel slot array antenna design is proposed, which is fed to the ESIW structure via a microstrip line. Power is moved via transition in this antenna from the microstrip to the ESIW structure. At 10 GHz, the antenna gain is 13.8 dB and the fractional bandwidth is 7.5%. The configured dimension is 222.75×40×4.4 mm^3. This design can be used in X-band radar applications. In this article, by reducing the size and modifying the structure geometry, impedance bandwidth has the optimal response in addition to a good result in efficiency and gain. The other advantage of antenna manufacturing by the PCB process is the high-power availability.

V. ACKNOWLEDGEMENTS

The authors acknowledge the Semnan University staff for their beneficial and professional help. Also, the authors would like to thank the journal editor and reviewers for their valuable comments.

DATA AVAILABILITY STATEMENT

Data sharing is not applicable to this article as no new data were created or analyzed in this study.

CONFLICT OF INTEREST

The authors declare no conflict of interests.

VI. REFERENCES

[1] Guha, D, Yahia M.M. Antar, YMM.: Microstrip and printed antennas: New trends, techniques and applications, John Wiley and Sons, First Edition, 2011.

[2] Fakharian, MM, Rezaei, P.: Very compact palmate leaf-shaped CPW-fed monopole antenna for UWB applications. Microw. Opt. Technol. Lett. 2014;56(7):1612-1616.

[3] Bhatti, R.A, Park, B.Y, et al.: Design of a planar slotted waveguide array antenna for X-band radar applications. J. Electromag. Eng. Sci. 2011;11: 97-104.

[4] Fakharian, MM.: A low-profile compact UWB antenna array for sub-6 GHz MIMO applications in 5G metal-frame smartphones. International Journal of RF and Microwave Computer-Aided Engineering. 2022; 32 (10): e23320.

[5] Khani, S, Vahab AL-Din Makki, S, et al.: Adjustable compact dual-band microstrip bandpass filter using T-shaped resonators. Microw. Opt. Technol. Lett. 2017;59(12):2970-2975.

[6] Mohammadi, B, Valizade Shahmirzadi, A, et al.: Design of a compact dual-band-notch ultra-wideband bandpass filter based on wave cancellation method. IET Microwaves, Antennas and Propagation, 2015; 9(1):1-9.

[7] Khani, S, Hayati, M. Compact microstrip lowpass filter with wide stopband and sharp roll-off. Microwave Journal. 2017; 60(11):86-92.

[8] Fakharian, MM.: RF energy harvesting using high impedance asymmetric antenna array without impedance matching network. Radio Sci. 2021;56(3):1-10.

[9] Shokouhi Shoormasti, A, Abbasi, A, Orouji, AA.:Using energy band engineering to improve heterojunction solar cells efficiency. Optik. 2020; 218:165243.

[10] Shirazi, S, Orouji, AA. Abbasi, A, Jafari SMH.: Improvement of Cd-free CIGS solar cell efficiency using triple silicon dioxide boxes as rear-passivation. Journal of Materials Science: Materials in Electronics. 2024; 35(6):1-12.

[11] Fakharian, MM.: A wideband fractal planar monopole antenna with a thin slot on radiating stub for radio frequency energy harvesting applications. International Journal of Engineering. 2020; 33(11):2181-2187.

[12] Kiani, S, Rezaei, P, Fakhr, M.: Dual-frequency microwave resonant sensor to detect non-invasive glucose level changes through the fingertip. IEEE Trans. Instrumentation and Measurement. 2021; 70:6004608.

[13] Jalalvand, AR, Rashidi, Z, et al.: Sensitive and selective simultaneous biosensing of nandrolone and testosterone as two anabolic steroids by a novel biosensor assisted by second-order calibration. Steroids. 2023; 189:109138.

[14] Khani, S, Hayati, M.: An ultra-high sensitive plasmonic refractive index sensor using an elliptical resonator and MIM waveguide. Superlatt. and Microstruct. 2021; 156:106970.

[15] Kiani, S, Rezaei, P, Navaei, M, Abrishamian, MS.: Microwave sensor for detection of solid material permittivity in single/multilayer samples with high quality factor. IEEE Sensors Journal. 2018; 18(24): 9971-9977.

[16] Alipour, AH, Khani, S, Ashoorirad, M, Baghbani, R.: Trapped multimodal resonance in magnetic field enhancement and sensitive THz plasmon sensor for toxic materials accusation. IEEE Sensors Journal. 2023; 23(13):14057-14066.

[17] Nimehvari Varcheh, H, Rezaei, P.: Low phase-noise X-band oscillator based on elliptic filter and branchline coupler. IET Microwaves, Antennas and Propagation. 2019; 13(7):888-891.

[18] Yang, Z, Luo, B, et al.: X-band low phase noise loop oscillator with differential outputs. Electron. Lett. 2015; 51(6):1005-1007.

[19] Varcheh, HN., Rezaei, P, Kiani, S.: A modified Jerusalem microstrip filter and its complementary for low phase noise X-band oscillator. International Journal of Microwave and Wireless Technologies. 2023; 15(10): 1707-1716.

[20] Karami, F, Rezaei, P, et al.: Efficient transition hybrid two-layer feed network: Polarization diversity in a satellite transceiver array antenna. IEEE Antennas Propag. Mag. 2021; 63(1):51-60.

[21] Le Sage, G.P.: 3D printed waveguide slot array antennas. IEEE Access, vol. 4 (2016), 1258-1265.

[22] Stern, G, Elliott, R.: Resonant length of longitudinal slots and validity of circuit representation: Theory and experiment. IEEE Trans. Antennas Propag., vol. 33 (1985), 1264-1271.

[23] Tyagi, Y, Mevada, P, et al.: High ‐ efficiency broadband slotted waveguide array antenna. IET Microwaves, Antennas and Propagation. 2017; 11: 1401-1408.

[24] Haghparast, A.H, Rezaei, P.: High performance H-plane horn antenna using groove gap waveguide technology. *AEU Int. J. Electron. Commun.*, vol. 163 (2023) 154620.

[25] Soleiman Meiguni, J, Ghobadi Rad, A.: WLAN substrate integrated waveguide filter with novel negative coupling structure. Modeling and Simulation on Electrical and Electronics Engineering (MSEEE). 2015; 1(2):15-18.

[26] Deslandes, D, Wu, K.:Integrated microstrip and rectangular waveguide in planar form. IEEE Microwave Wireless Component Letters, 2001; 11:68-70.

[27] Weng, Q, Lin, Q, Wu, H. The propagation characteristics of rectangular waveguides filled with inhomogeneous double-negative dielectrics using a semianalytical method. International Journal of Numerical Modelling. 2021; 34: e2860.

[28] Mohammadi, B, Valizade, A, et al.: New design of compact dual band-notch ultra-wideband bandpass filter based on coupled wave canceller inverted T-shaped stubs. IET Microwaves, Antennas and Propagation. 2015; 9(1):64-72.

[29] Nasrabadi, E, Rezaei, P. A novel design of reconfigurable monopole antenna with switchable triple band-rejection for UWB applications. International Journal of Microwave and Wireless Technologies, vol. 8, (2016), 1223-1229.

[30] Khani, S, Danaie, M, et al.: Compact ultra-wide upper stopband microstrip dual-band BPF using tapered and octagonal loop resonators. Frequenz, vol. 74 (2020), 61-71.

[31] Kiani, S, Rezaei, P, Navaei, M.: Dual-sensing and dual-frequency microwave SRR sensor for liquid samples permittivity detection. Measurement. 2020; 160:107805.

[32] Kiani, N, Afsahi, M, et al.: Implementation of a fourth-order compact quasi-elliptic substrate integrated waveguide filter in C-band. Modeling and Simulation on Electrical and Electronics Engineering (MSEEE). 2022; 2(2):23-27.

[33] Karami, F, Boutayeb, H, et al.: Multifunctional switched-beam antenna located on solar cell for vehicular to satellite communication. IEEE Trans. Vehicular Technol. 2024; 73(3): 3457-3468.

[34] Kiani, S, Rezaei, P, et al.: Substrate integrated waveguide quasi-elliptic bandpass filter with parallel coupled microstrip resonator. Electron. Lett., vol. 54, (2018), 667-668.

[35] Hirokawa, J, Ando, M.: Efficiency of 76-GHz post-wall waveguide-fed parallel-plate slot arrays. IEEE Trans. Antennas Propag., vol. 48 (2000), 1742-1745.

[36] Kiani, S, Rezaei, P.: Microwave substrate integrated waveguide resonator sensor for non-invasive monitoring of blood glucose concentration: Low cost and painless tool for diabetics. Measur. 2023; 219:113232.

[37] Fakharian, MM.: A dual circular and linear polarized rectenna for RF energy harvesting at 0.9 and 1.8 GHz GSM bands. *Electromagnetics.* 2021; 41(8):545-556.

[38] Xiao, S, Yang, L.: T-type folded SIW-based leaky-wave antennas with wide scanning angle and low cross-polarization. International Journal of Microwave and Wireless Technologies, vol. 14 (2022), 949-954.

[39] AmneElahi, A, Rezaei, P, et al.: Analysis and design of a stacked PCBs-based quasi-helix antenna. IEEE Trans. Antennas Propag., vol. 70 (2022), 12253-12257.

[40] Khatami, S.A, Meiguni, et al.: Compact via-coupling fed monopulse antenna with orthogonal tracking capability in radiation pattern. IEEE Antennas Wirel. Propag. Lett., vol. 19 (2020), 1443-1446.

[41] Li, L, Yan, J.B.: A low-cost and efficient microstrip-fed air-substrate-integrated waveguide slot array. Electronics, vol. 10 (2021), 338.

[42] Al Khanjar, K, Djerafi, T.: Partially dielectric-filled empty substrate integrated waveguide design for millimeter-wave applications. Progress in Electromagnetics Research C., vol. 87 (2018), 135-146.

[43] Wang, Y, Yang, X.X, et al.: Study on millimeter-wave SIW rectenna and arrays with high conversion efficiency. IEEE Trans. Antennas Propag., vol. 69 (2021), 5503-5511.

[44] Abdi Diman, A, Karami, F, et al.: Efficient SIW-feed network suppressing mutual coupling of slot antenna array. IEEE Trans. Antennas Propag., vol. 69 (2021), 6058-6063.

[45] Freeman, J.C.: Fundamentals of microwave transmission lines. New York: Wiley, 1996.

[46] Mateo, J, Torres A.M, et al.: Highly efficient and well-matched empty substrate integrated waveguide H-plane horn antenna. IEEE Antennas Wirel. Propag. Lett., vol. 15 (2016), 1510-1513.

[47] Khan, Z.U, Jilani, S.F, et al. Empty substrate integrated waveguide-fed MMW aperture-coupled patch antenna for 5G applications. EuCAP., arXiv e-prints (2018), arXiv-1809.

[48] Nigam, P, Muduli, A, et al.: SIW based cavity backed self-quadplexing slot antenna. J. Microw. Optoelectron. Electromag. Appl., vol. 20 (2021), 490-503.

[49] Xu, J, Chen, Z.N, Qing, X.: CPW center-fed single-layer SIW slot antenna array for automotive radars. IEEE Trans. Antennas Propag., vol. 62 (2014), 4528-4536.

[50] Yan, L, Hong, W, et al.: Simulation and experiment on SIW slot array antennas. IEEE Microw. Wireless Compon. Lett., vol. 14 (2004), 446-448.

[51] Parment, F, Ghiotto, A, et al.: Millimetre-wave air-filled substrate integrated waveguide slot array antenna. Electron. Lett., vol. 53 (2017), 704-706.